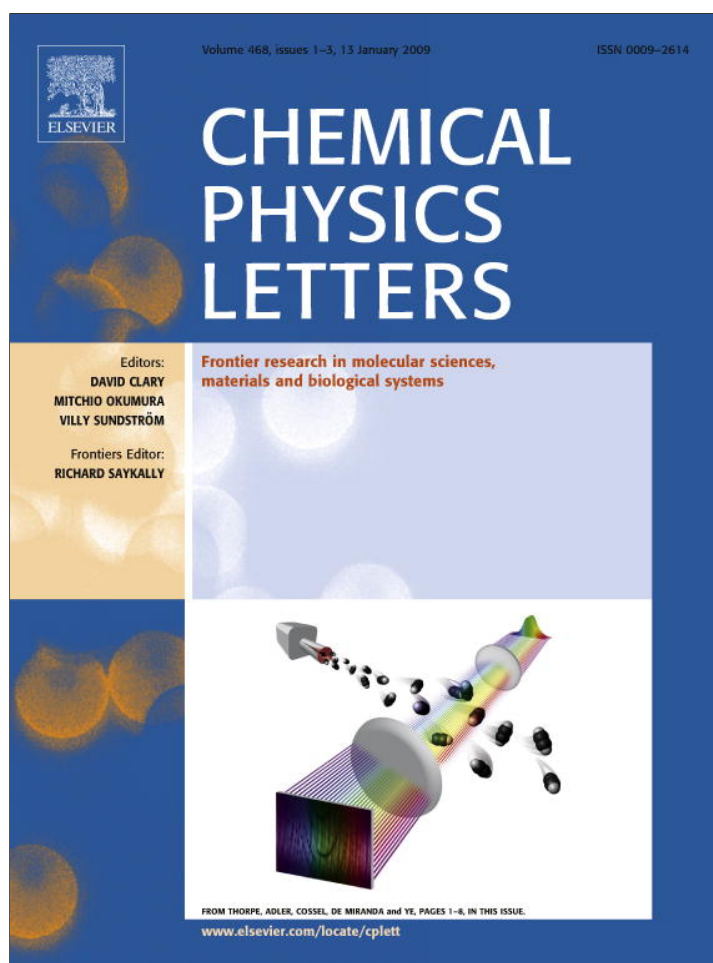


Provided for non-commercial research and education use.  
Not for reproduction, distribution or commercial use.



This article appeared in a journal published by Elsevier. The attached copy is furnished to the author for internal non-commercial research and education use, including for instruction at the authors institution and sharing with colleagues.

Other uses, including reproduction and distribution, or selling or licensing copies, or posting to personal, institutional or third party websites are prohibited.

In most cases authors are permitted to post their version of the article (e.g. in Word or Tex form) to their personal website or institutional repository. Authors requiring further information regarding Elsevier's archiving and manuscript policies are encouraged to visit:

<http://www.elsevier.com/copyright>



Contents lists available at ScienceDirect

## Chemical Physics Letters

journal homepage: [www.elsevier.com/locate/cplett](http://www.elsevier.com/locate/cplett)

## A time constant of 1.8 fs in the dissociation of water excited at 162 nm

Sergei A. Trushin, Wolfram E. Schmid, Werner Fuß\*

Max-Planck-Institut für Quantenoptik, Hans-Kopfermann Straße 1, D-85748 Garching, Germany

## ARTICLE INFO

## Article history:

Received 24 October 2008

In final form 28 November 2008

Available online 7 December 2008

## ABSTRACT

Probing the first excited-state of H<sub>2</sub>O, HDO and D<sub>2</sub>O by ionization at 810 nm reveals in the parent-ion yields time constants of 1.8, 2.1 and 2.5 fs, respectively, during which the molecule leaves the Franck–Condon region, stretching the bonds of by about 0.25 Å. The OH<sup>+</sup> signal rises slightly more slowly (1.8 + 1.7 fs), because only then is the dissociation energy of the parent ion overcome. The subsequent decay (3.3 fs) is caused by the decreasing ionization probability. The detection of such short times is intimately connected with the sensitivity of the probe technique to geometrical changes in the sub-Ångström range.

© 2008 Elsevier B.V. All rights reserved.

## 1. Introduction

Photodissociation of water via its first absorption band ( $\tilde{A}^1B_1$ ) near 166 nm has been much studied, also because it is the prototype of bond cleavage on a directly repulsive potential energy surface (PES). The knowledge on the process, the PES and the experimental techniques have been reviewed by Engel et al. [1] and in the book by Schinke [2], briefly also in [3,4]. The molecule is small enough to allow the PES for the excited state to be calculated with high quality as a function of all coordinates. The most widely used PES is that of Staemmler and Palma [5] (see also [6]), which has only recently been slightly improved by van Harreveld and van Hemert [7,8]. These potentials have been tested with extensive experimental investigations (see the reviews): the ( $\tilde{X} \rightarrow \tilde{A}$ ) absorption spectrum with its diffuse vibrational structure [9] and the  $\tilde{C} \rightarrow \tilde{A}$  emission spectrum, the population of rotational, vibrational and electronic states of the product OH without and with initial rotational-vibrational excitation, the OH/OD branching ratio in dissociation of HDO and the resonance Raman spectra. Only recently have photofragment translational spectra of the product H become available [10–12].

Time-resolved monitoring of water photodissociation can also give information on the shape of the potentials. Such measurements have been attempted by Farmanara et al. [13,14]; but due to the limited time resolution ( $\geq 300$  fs) only an upper bound (20 fs) could be given for the dissociation time. An  $\tilde{A}$  lifetime of 40 fs was estimated from vector correlations in dissociation of rotationally excited H<sub>2</sub>O [15]. From calculated wave packet dynamics it was concluded that the dissociation is complete after 25 fs [16]. From the width of the absorption spectrum an excited-state lifetime of 5 or 8 fs has been estimated [17,18]. For the calculated decay of the autocorrelation function, see below.

Of course, dissociation is a continuous process, and the measured time for it depends on the limits of the observation window of the probing process. Nonresonant ionization for probing with mass-selective detection of the ion yield usually [19] – also in the case at hand – can detect several consecutive such windows. In the present case, we assign the first to the Franck–Condon (FC) region (departure within 1.8 fs), the end of the second to an OH distance where ionization leads to an energy higher than the dissociation limit of H<sub>2</sub>O<sup>+</sup>, whereas the third is characterized by the steep decrease of the ionization probability of H<sub>2</sub>O along the OH stretch coordinate.

## 2. Experimental

Vapors of H<sub>2</sub>O, D<sub>2</sub>O and HDO (the latter from a liquid mixture of H<sub>2</sub>O and D<sub>2</sub>O) at pressures of  $10^{-7}$ – $10^{-5}$  mbar were excited in the ionization region of a time-of-flight mass spectrometer by the fifth harmonic (162 nm, 10 fs,  $10^{10}$  W cm<sup>-2</sup>) of a Ti-sapphire laser, whose fundamental (810 nm, 12 fs,  $\approx (3-10) \times 10^{13}$  W cm<sup>-2</sup>) served for probing by nonresonant ionization. The shortening of the fundamental is described in [20] and the generation of the fifth harmonic in [21]; for a brief description see also [22]. The pump-probe delay was varied in steps of 3.3 fs. The time zero is derived from the maximum of the Xe<sup>+</sup> signal (from added Xe) measured in every pulse together with the H<sub>2</sub>O<sup>+</sup> or OH<sup>+</sup> signal. For HDO and D<sub>2</sub>O, only the parent ion was investigated, because their fragment ions would coincide with signals from background water. The signals (time-dependent ion yields) are evaluated by fitting to them a sum of exponentials, convoluted with the instrumental function; for the latter we take a Gaussian of full width at half maximum of 11 fs, which is the convolution of the pump pulse (9.7 fs) with the fourth or a higher power of the probe pulse (12 fs). The Gaussian shape was confirmed down to about  $10^{-2}$  of the maximum of the H<sub>2</sub>O<sup>+</sup> signals (see below). Details of the technique – time-resolved intense field dissociative ionization – including

\* Corresponding author. Fax: +49 89 32905 200.

E-mail address: [w.fuss@mpq.mpg.de](mailto:w.fuss@mpq.mpg.de) (W. Fuß).

evaluation are given, for example, in Ref. [19]. The use of rate equations (i.e. exponential fitting) is normally not expected to be suitable for wave packet dynamics; however, it is justified in [22–25] by the fact that the observation windows are broad.

Both lasers were linearly polarized, parallel to each other and to the axis of the time-of-flight mass spectrometer. In principle, one could use the magic angle ( $55^\circ$ ) between the two polarizations to avoid effects due to rotation of the molecule. However, rotational anisotropy would show time-dependent effects on a much longer time scale (35–60 fs, calculated at 295 K as in [26] from the moments of inertia) than the time constants found here, so that there was no necessity to choose such an angle.

### 3. Results

Fig. 1 shows the delay-time-dependent yields of  $\text{H}_2\text{O}^+$  together with those of  $\text{Xe}^+$ . The smooth curves are simulations of the data by Gaussians: The  $\text{Xe}^+$  data should represent the cross-correlation of the UV pulse with the third power of the IR probe pulse, because ionization (12.13 eV) requires one UV photon (7.65 eV) plus  $m = 3$  IR photons (1.53 eV). Their fit curve should be the instrumental function: The width of this function ( $\tau_{\text{instr}} = (\tau_{\text{pu}}^2 + \tau_{\text{pr}}^2/m)^{1/2}$ )

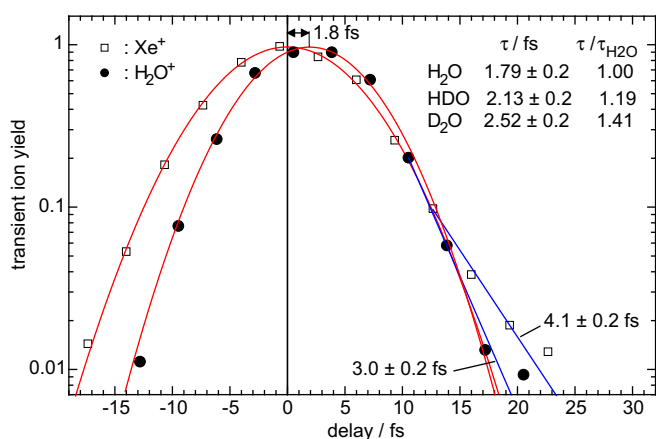


Fig. 1. Parent-ion signal of  $\text{H}_2\text{O}$  (circles) and the  $\text{Xe}^+$  signal. The latter defines the time zero. The  $\text{Xe}^+$  simulation is Gaussian, except in the tail (also of  $\text{H}_2\text{O}^+$ ), where an exponential is used. The  $\text{H}_2\text{O}^+$  simulation is a convolution of a Gaussian (instrumental function, width 11 fs) with one or two exponentials ( $\tau_1$ ,  $\tau_2$ ); in the latter case, contributions were assumed in a ratio of 20:1 from  $L_1$  and  $L_2$ . The two simulations are not distinguishable. The table lists the  $\tau_1$  values for the three isotopomers. The error limits are the standard deviation of the average values in 10 runs.

just scarcely depends on  $m$  [19] if ionization needs  $m \geq 3$  IR photons. (Water with its ionization energy of 12.62 eV from the ground state requires 9 photons, from the FC region 4, and  $>4$  from later locations on the PES.) The upper part ( $\geq 3\%$  of the maximum) of the  $\text{Xe}^+$  data is well fitted by a Gaussian with a width of 13 fs. The corresponding part of  $\text{H}_2\text{O}^+$  is narrower (11 fs). We interpret the larger width of the  $\text{Xe}^+$  data by assuming a lower effective order for Xe ionization. Such a phenomenon can happen if a real intermediate state is involved whose population or depopulation is very fast (partially saturated by the strong IR pulse). (For example, the  $7s$  state at  $85\,189\text{ cm}^{-1}$  can probably be populated by one UV + two IR photons.) Only on the assumption of an effective order for Xe ionization of  $m \approx 2$  can one simultaneously fit the narrower width of the  $\text{H}_2\text{O}^+$  signal. These fits imply a UV pulse duration of 9.7 fs.

Deviations from a Gaussian are observed at lower signal levels and are simulated in Fig. 1 by exponential decays with time constants 4 fs for  $\text{Xe}^+$  and 3 fs for  $\text{H}_2\text{O}^+$  (Fig. 1). This means that the UV pulse (therefore certainly also the IR pulse) is not purely Gaussian. In fact the  $\text{Xe}^+$  and  $\text{H}_2\text{O}^+$  signals both have a weak satellite ( $\approx 0.2\%$  of the maximum near 35–40 fs, as is seen in data covering this range), and the dip before the satellite is obviously less well resolved in the  $\text{Xe}^+$  data due to the lower order of ionization.

The exponential slope (or deviations from a Gaussian) in the weak, decaying wing of the instrumental function also implies that time constants  $\leq 3$  fs cannot be determined from this wing; it only provides an upper bound of  $\tau_1 \leq 3$  fs. (Because  $\text{D}_2\text{O}^+$  exhibits the same slope, the upper bound for  $\text{H}_2\text{O}$  can be sharpened by a factor of 1.4 to  $\tau_1 \leq 2.1$  fs.) However, the lifetime can also be evaluated from the Gaussian part: By simulating this earlier part by a convolution of a Gaussian (width 11 fs) instrumental function with an exponential (fit parameter  $\tau_1$ ), we find a lifetime  $\tau_1 = 1.8$  fs. It is also the origin of the 1.8 fs delay of the maximum. Such a deconvolution requires some caution, because there can be nonlinear complications during the overlap of the high-intensity probe with the pump pulses [27]. However, two confirmations that  $\tau_1$  is real can be seen (1) in the fact that it is found to be 1.4 times larger in  $\text{D}_2\text{O}$  ( $\sqrt{2}$  is the expected deuterium isotope effect for a barrierless process) and in between with HDO (both signals not shown), and (2) in the upper bound ( $\tau_1 \leq 2.1$  fs) found above from the decaying wing.

Fig. 2 shows the data for the fragment  $\text{OH}^+$ . If they are fitted with a rise time of 1.8 fs (taken from the parent ion) and a decay (with convolution with the instrumental function) there is a noticeable deviation of an oscillatory form. In fact, the simulation is much improved if the sum of the two exponentials (with convolution) is multiplied by a periodic function (see, for example, [22])

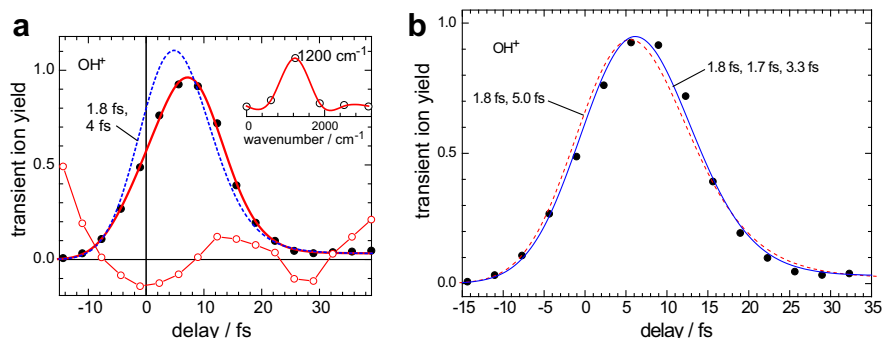


Fig. 2. Fragment-ion signal ( $\text{OH}^+$ , solid symbols): (a) simulated with two exponentials, convoluted with a Gaussian instrumental function (broken line) and multiplied by the periodic function  $f_{\text{osc}}$  (solid line); the open symbols show the data divided by the exponential part diminished by 1 ( $=f_{\text{osc}} - 1$  ideally) and the inset its Fourier (power) spectrum. In (b) the data are simulated with two (broken line) and three (solid line) exponentials, convoluted with the instrumental function. In both simulations the fragment ion is produced only from the last observation window.

$$f_{\text{osc}} = 1 + A \cos(2\pi\nu t - \varphi) \quad (1)$$

with period 28 fs (corresponding to a wavenumber of  $1200 \text{ cm}^{-1}$ , if interpreted as a molecular vibration). This is shown in Fig. 2a; the fitted decay is then 4 fs. However, in the next section we argue that a better analysis uses an additional time constant instead of the periodic modulation. Fig. 2b compares two purely exponential simulations (with convolution), one (broken line) using a singly exponential rise (1.8 fs) with a decay (5 fs), the other (solid line) with two consecutive processes rising with  $\tau_1 = 1.8 \text{ fs}$  and  $\tau_2 = 1.7 \text{ fs}$ , followed by a decay with  $\tau_3 = 3.3 \text{ fs}$ . (Because the simulation in Fig. 2a was done including the oscillatory function, its exponential part does not coincide with the broken line in Fig. 2b.) In Fig. 2b inclusion of a third time constant slightly improves the fit. In both simulations we assumed that the fragment ion is produced only from the last observation window.

The fragment signal decays to a level which is initially (for example, near 35 fs, Fig. 2) 4% of the maximum but then decays within 100 fs to a pedestal. However, this part was found to depend on the square of the pump intensity (whereas the preceding parts are linear in it). That is, the ions in this part are produced by two pump photons and subsequent fragmentation by the probe. The 100 fs component and the pedestal hence do not represent one-photon photochemistry and can be subtracted. (Probably ionization by the two UV photons populates both the  $\tilde{X}$  and  $\tilde{A}$  states of the ion. The latter merges with the former at a bend angle of  $180^\circ$  [28]. The time-dependent signal may hence represent  $\tilde{A} \rightarrow \tilde{X}$  relaxation, whereas the pedestal may be due to the stable ground state  $\tilde{X}$ .) The residual after subtraction of the UV-intensity-dependent signal coincides with 0 within the noise level. That is, the neutral OH fragment is below the detection limit.

#### 4. Discussion

The  $\tilde{A}$  surface of water is shown by the contour lines of Fig. 3 (adapted from [5,18]). It is repulsive along each OH distance. On vertical excitation (to the 'FC point' in Fig. 3) the initial acceleration is towards a symmetric stretch. The trajectory then bends towards antisymmetric stretching and thereafter to cleavage of a single OH bond, as indicated. The total energy release is 2.5 eV, with about 2.0 eV in translation (corresponding to  $20 \text{ km s}^{-1} = 0.2 \text{ \AA fs}^{-1}$  of the H atom) and practically all the rest in vibration of the OH fragment (see the numbers in [10–12]). There is no (or according to

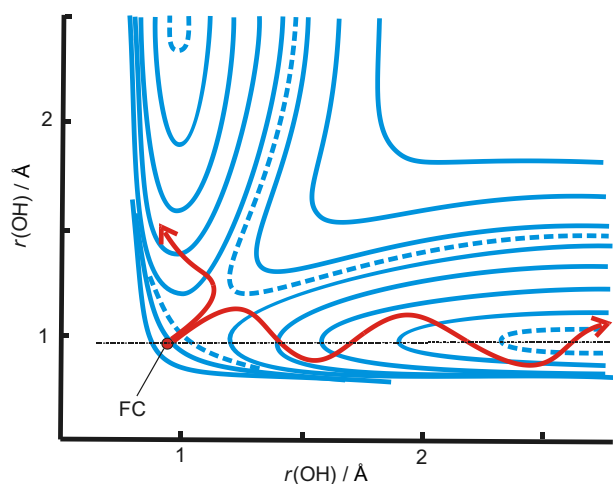


**Fig. 3.** Potential of water in its  $\tilde{A}$  state along the two OH distances (from [5]) and path of the wave packet. The solid contour lines have a distance of 0.5 eV, and the distance to the broken lines is 0.25 eV. The dotted horizontal line indicates the direction of the cut shown in Fig. 4.

[12] almost no) bending involved, because the HOH angle is unchanged in the  $\tilde{A}$  state and the potential becomes very flat in this direction on OH stretching [1,2,5].

The wave packet on the  $\tilde{A}$  surface is monitored by ionization with varied delay of the probe. This process requires more and more photons, because the ion is strongly bound (dissociation energy 5.39 eV [29]); that is, the neutral ( $\tilde{A}$ ) and ionic (ground state) potentials separate more and more on increasing an OH distance (from 5.0 eV in the FC region to a final value of 12.9 eV). The ionization is vertical (preserves the atomic distances). It also does not change the translational momentum (within the uncertainty principle). Hence probing gives rise to an ion with excess energy (above the local electronic energy) equal to the local nuclear kinetic energy of the neutral molecule. In Fig. 4 this is shown along a one-dimensional cut by the broken line. This line crosses the ionic dissociation limit at an OH distance of 1.70  $\text{\AA}$ . Beyond this distance, the molecular ion should not be observable anymore.

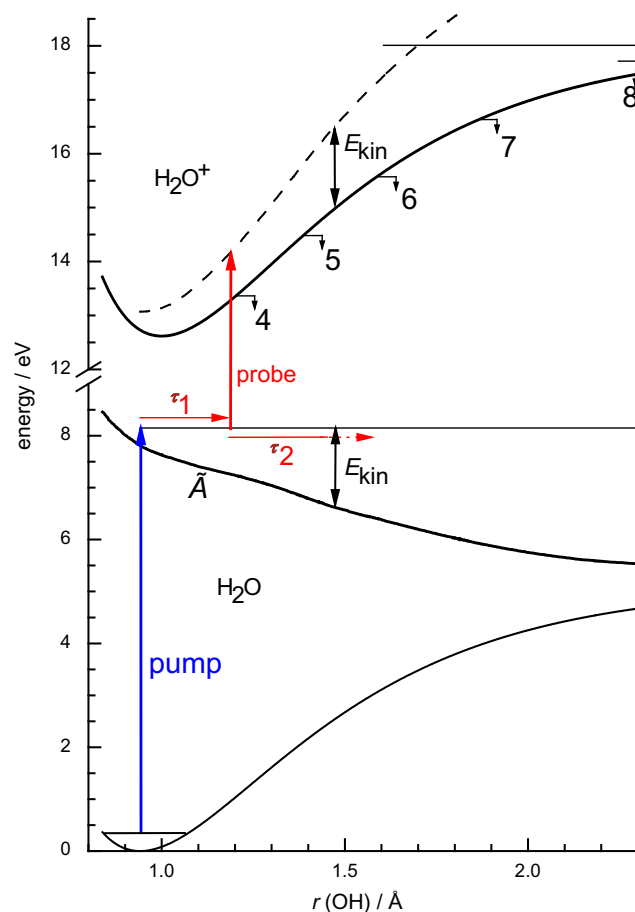


**Fig. 4.** Cut (along the dotted line in Fig. 3) of the potentials of  $\text{H}_2\text{O}$  and  $\text{H}_2\text{O}^+$ . The line for  $\tilde{A}$  is from the calculation of [8]. For  $\text{H}_2\text{O}^+$  we took a Morse function  $E = E_{\text{diss}} (1 - \exp(-(r-r_0)/r_{00}))^2$  with a minimum at  $r_0 = 1.00 \text{ \AA}$ , a width of  $r_{00} = 0.436 \text{ \AA}$  [34] and a dissociation energy of  $E_{\text{diss}} = 5.39 \text{ eV}$  [29]. For the ground state of  $\text{H}_2\text{O}$  we took a Morse curve with the same  $r_{00}$  but  $r_0 = 0.941 \text{ \AA}$  and  $E_{\text{diss}} = 5.113 \text{ eV}$  [29]. The initial kinetic energy after excitation by the pump is assumed to be  $=0.34 \text{ eV}$ , the change of the zero-point energy. The broken line is the ionic potential energy plus the kinetic energy of the neutral (as indicated by the double arrows). The energy levels up to which  $m = 4-8$  photons are sufficient to reach the ion from the neutral  $\tilde{A}$  state are also indicated. We suggest that dissociation of  $\text{H}_2\text{O}^+$  already begins near the double arrow (via an excited ionic state) but is completed only after the crossing of the broken line (=potential + kinetic energy) with the asymptote. We assume that the limit of the observation window  $L_1$  (arrow labeled ' $\tau_1$ ') is primarily given by the FC integral (Eq. (2)) or the zero-point amplitude, which accidentally nearly coincides with the limit, up to which 4 probe photons are sufficient for ionization; the former is a molecular constant, whereas the latter would depend on the photon energy.

(Hence this probing technique defines a sharp limit of dissociation.) We can check with the calculated potentials whether the wave packet can reach this point within the measured times. Our measurements thus may provide another examination of the potentials.

This is done here by a (rough) classical calculation: The kinetic energy (double arrow in Fig. 4) is converted to a velocity  $dr/dt$  ( $r = \text{OH}$  distance, reduced mass  $\approx 1$  u), whose inverse  $dt/dr$  is integrated over the distance, the result representing  $t(r)$ . We find that the dissociation distance (1.70 Å) is reached after a time of  $\approx 5.4$  fs. This agrees only poorly with our  $\tau_1 + \tau_2$  ( $\approx 3.5$  fs), a time during which the  $\text{OH}^+$  signal appears (Fig. 2b). A more sophisticated consideration takes into account that after some OH stretching the ion can be resonantly excited by the probe to its  $\tilde{A}$  state, so that the dissociation threshold can be reached earlier. On adding the energy of one probe photon (1.53 eV) to the broken line in Fig. 4, one finds that then the dissociation energy is already reached at 1.47 Å (at the position of the double arrows). This distance is reached after 4.1 fs, in better agreement with our  $\tau_1 + \tau_2$ . We hence suppose that ionic dissociation at early times involves the first excited state of  $\text{H}_2\text{O}^+$  and is completed at later times (after  $\geq 5.4$  fs) via its ground state. It is conceivable that with shorter pulses one could distinguish one more window between  $L_2$  and  $L_3$ . Improvements of the calculation should involve two dimensions and take for the ion a more accurate potential (which is simplified in Fig. 4). With such a better ionic potential, a critical check for the  $\tilde{A}$  potential may be provided by quantum-dynamical calculations for the motion on this potential in two dimensions (see Eq. (2) below). But the rough classical calculation is sufficient to confirm that indeed the  $\text{OH}^+$  signal must be analysed by the longer appearance time ( $\tau_1 + \tau_2$ , solid line in Fig. 2b) instead of using only  $\tau_1$  (broken line in Fig. 2b) and perhaps an oscillatory modulation (Fig. 2a). The fact that the fit in Fig. 2b is slightly less perfect than in Fig. 2a may indicate that such a small molecule can deviate to some extent from purely exponential (statistical) behavior.

However, if the  $\text{OH}^+$  signal appears within 3.5 fs, how can the  $\text{H}_2\text{O}^+$  signal disappear faster (in 1.8 fs, Fig. 1)? Here it should be realized that the decrease of the molecular-ion yield has two origins: besides dissociation of the primary ion (as above), the decrease of ionization probability (due to the steep rise of ionization energy and the loss of FC overlap, see below). If the probability difference at early and later times is large enough (for example, by a factor  $\geq 20$ ), one can define two observation windows (ranges or locations  $L_1, L_2$  on the PES) for the parent ion: In the first, characterized by  $\tau_1$ , the molecule is ionized by four probe photons, and by more in the second (Fig. 4), and only after the second is the dissociation threshold of the ion overcome (see above). The much smaller ionization probability from  $L_2$  (assumed: 5% of that of  $L_1$ ) explains why  $\tau_2$  cannot be detected in the parent-ion yield (Fig. 1: the simulation curves with and without  $L_2$  are indistinguishable). (In contrast, the  $\text{OH}^+$  signal is weak already from the beginning: near time 0 it is only 5% of the parent ion.)

The observation window  $L_1$  is not only limited by the electronic transition probability (which drops, where 4 photons are no longer sufficient for ionization, which is near the arrow 'probe' in Fig. 4) but also by the FC overlap of the nuclear wave functions. In a time-dependent picture, this is the autocorrelation function,

$$C_{\text{ioniz}}(t) = \langle \chi_i | \chi(t) \rangle \quad (2)$$

where the brackets indicate spatial integration,  $\chi_i$  is the ground vibrational wave function of the ion and  $\chi(t)$  is the wave packet of the neutral on its way to dissociation. The latter can be calculated from  $\chi(0) = \chi_{\text{gs}}$  (ground state wave function of  $\text{H}_2\text{O}$ ) by propagation with the help of the  $\tilde{A}$  potential. This is the same formalism as in the description of absorption from the neutral ground state [18,30]. A calculation of (2) is not available. However, the ion potential is very

similar to that of the neutral ground state (nearly the same OH distance, force constants and dissociation energies). It is therefore a good approximation to take instead of  $C_{\text{ioniz}}$  the corresponding function  $C_{\text{abs}}$  for absorption from the ground state, with  $\chi_{\text{gs}}$  instead of the ionic  $\chi_i$ . This function  $C_{\text{abs}}$  has been calculated by Henriksen et al. [18]. An inspection of Fig. 3 of [18] shows that this  $C_{\text{abs}}$  decays to  $e^{-1}$  within 2.2 fs (though not perfectly exponentially: to  $e^{-2}$  in 3.3 fs =  $2 \times 1.65$  fs), in good agreement with our  $\tau_1 = 1.8$  fs. If  $\chi(t)$  has a constant width, the integral (2) decays to  $e^{-1}$  over a distance change equal to this width, which is the zero-point vibrational amplitude ( $\approx 0.20$  Å for each OH, as indicated in Fig. 4); the actual decay takes only marginally longer. We should mention that the control by the FC integral is only valid for probe wavelengths near the threshold of ionization (considering the ion yield as a function of the photon energy); with much more energetic photons ( $\gg 6$  eV), the yield becomes independent of this integral, because the sum of FC factors (which is = 1) must be taken. This is derived in detail for one-photon ionization in [31].

The  $\text{OH}^+$  signal decays to 0 within  $\tau_3 = 3.3$  fs. This is obviously due to the steep rise of the ionization potential in  $L_3$ , i.e., on stretching the OH bond (Fig. 4). Free OH is not detected, owing to its ionization energy of 12.9 eV, which would require 9 probe photons for ionization.

The calculated autocorrelation function  $C_{\text{abs}}(t)$  of the wave packet after absorption from the ground state shows a weak ( $\approx 3\%$  of the maximum) recurrence around 19 fs after absorption [18]. It corresponds to the symmetric stretch vibration (diagonal in Fig. 3) in the FC region ( $L_1$ ), which also shows up in the absorption spectrum as a weak modulation (wavenumber  $\approx 1850$   $\text{cm}^{-1}$  [9]). Such a weak revival would be located far in the tail of the parent-ion signal and cannot be detected there because of the irregularity in the decaying part of the pulse (deviation from a Gaussian shape, Fig. 1). (The example also demonstrates that for extracting short-time phenomena, it is desirable to have not only short half-widths but also clean shapes without satellites or tails.)

This vibration is not expected to modulate the  $\text{OH}^+$  signal, because  $\text{OH}^+$  does not arise from  $L_1$  but only from  $L_3$ . This already casts doubt on the first alternative (Fig. 2a) of evaluation of the  $\text{OH}^+$  signal, which suggested an oscillation of  $1200$   $\text{cm}^{-1}$ . This wavenumber also would not fit to the HOH bend ( $\approx 690$   $\text{cm}^{-1}$ , calculated from the bend potential of [7] in the FC region), although perhaps to an overtone after some OH stretching. However, the modulation in Fig. 2a begins with negative amplitude, although the ionization probability should be highest in the initial location along the bending coordinate, as is to be concluded from the relative energies of the flat neutral and steep ion PES. Since the  $1200$   $\text{cm}^{-1}$  also disagree with the OH stretch during or after dissociation ( $3728$   $\text{cm}^{-1}$ ), and because also the classical calculation suggested a time much larger than  $\tau_1$  to reach the dissociation distance, we drop the two-time constant approach and prefer the evaluation with three time constants (solid line in Fig. 2b), as discussed above. The data alone could not decide which analysis to prefer.

## 5. Concluding remarks

The first time constant ( $\tau_1 = 1.8$  fs for  $\text{H}_2\text{O}$ ) was directly measured, although the evaluation required deconvolution. It is confirmed by the deuterium isotope effect and by the upper bound ( $\tau_1 \leq 2.1$  fs for  $\text{H}_2\text{O}$ ) derived from the decaying wing of the parent-ion signal. It also agrees with the calculated time taken to leave the FC region. In contrast, there is no compelling evidence for  $\tau_2$  from the time-dependent data alone, although it is consistent with them: With the assumption of such a step, one obtains a simulation curve for the  $\text{OH}^+$  signal which is only slightly better (slightly

delayed) in relation to that without this constant (Fig. 2b); a higher time resolution could decide. But such an intermediate step must be assumed, because there is no chance that the wave packet can reach within 1.8 fs a location (an OH bond extension) where the ion dissociates (Fig. 4).

The constant  $\tau_1$  is to our knowledge the shortest time ever measured directly in a time-resolved experiment for nuclear dynamics. (The varying line widths of the  $\tilde{C} \rightarrow \tilde{A}$  emission [16] imply that these lifetimes depend on the excess energy in the  $\tilde{A}$  state.) The previously reported shortest time is based on indirect evidence (line width of emission spectra): It was suggested that dissociation of  $H_3$  takes 3.5 fs and 6.7 fs from the lower and upper sheet of the Jahn-Teller-split ground state surface [32]. By direct time resolution we also found time constants of 4 fs in dissociation of oxygen [33] and of 188tfs in dissociation of  $Cr(CO)_6$  [27].

As already said, during  $\tau_1$  the hydrogen is not fully cleaved off but moves by only a fraction of an Ångström, and similarly also within  $\tau_2$  and  $\tau_3$ . The PES is thus sampled over consecutive small ranges, a result of the short pulses and a high spatial resolution of the probe technique. The latter in the given case is due (1) in  $L_1$  to the compactness (zero-point amplitude) of  $\chi_i$  (vibrational wave function in the ground state of the ion), (2) in  $L_2$  from the sudden overcoming of the ionic dissociation threshold, and (3) in  $L_3$  from the steep rise of the ionization energy (decrease of the ionization probability). These three features are all based on the strongly bound ion potential. One can expect similar cases with compounds, which are also photodissociated via an  $n \rightarrow \sigma^*$  excitation and probed via an ion with a hole in the n orbital. Obvious examples are the hydrogen halides or the molecules reviewed in [3]; but heavier molecules can also be considered, because their zero-point amplitude is smaller, so that the better spatial resolution may compensate the slower motion. Because the (bound) PESs of the ion are known or accessible by spectroscopic techniques with high precision, the repulsive surface of the neutral can be derived from time-resolved data as suggested above, together with quantum-dynamical calculations, using Eq. (2) for the FC region and an extension of it outside.

One can ask whether shorter-time nuclear dynamics is also conceivable and detectable. For this purpose, a wave packet of correspondingly short duration must be prepared by a suitable pump pulse; this is limited by the width of the absorption spectrum: in water molecules to about 0.6 fs and in the hydrogen halides to about 0.4 fs. During such a time, the wave packet only moves by a fraction of an Ångström. Similarly, as demonstrated in this work,

consideration of the PES involved in probing must show whether there is sufficient change of signals over the correspondingly short distances that the probe technique can resolve such short times.

## Acknowledgement

This work was supported by the Deutsche Forschungsgemeinschaft (Project FU 363/1).

## References

- [1] V. Engel et al., *J. Phys. Chem.* 94 (1992) 3201.
- [2] R. Schinke, *Photodissociation Dynamics*, Cambridge University Press, Cambridge, 1993.
- [3] M.N.R. Ashfold, D.H. Mordaunt, S.H.S. Wilson, *Adv. Photochem.* 21 (1996) 217.
- [4] M.B. Robin, *Higher Excited States of Polyatomic Molecules*, vol. 3, Academic Press, New York, 1985.
- [5] V. Staemmler, A. Palma, *Chem. Phys.* 93 (1985) 63.
- [6] G. Theodorakopoulos, I.D. Petsalakis, R.J. Buenker, *Chem. Phys.* 96 (1985) 217.
- [7] R. van Harrevelt, M.C. van Hemert, *J. Chem. Phys.* 112 (2000) 5777.
- [8] R. van Harrevelt, M.C. van Hemert, *J. Chem. Phys.* 114 (2001) 9453.
- [9] H.T. Wang, W.S. Felps, S.P. McGlynn, *J. Chem. Phys.* 67 (1977) 2614.
- [10] D.W. Hwang, X. Yang, X. Yang, *J. Chem. Phys.* 110 (1999) 4119.
- [11] X.F. Yang, D.W. Hwang, J.J. Lin, X. Ying, *J. Chem. Phys.* 113 (2000) 10597.
- [12] I.C. Lu, F. Wang, K. Yuan, Y. Cheng, X. Yang, *J. Chem. Phys.* 126 (2008) 066101.
- [13] P. Farmanara, O. Steinkellner, M.T. Wick, M. Wittmann, G. Korn, V. Stert, W. Radloff, *J. Chem. Phys.* 111 (1999) 6264.
- [14] M. Wittmann et al., *Opt. Comm.* 173 (2000) 323.
- [15] I. Bar, D. David, S. Rosenwaks, *Chem. Phys.* 187 (1994) 21.
- [16] J.Z. Zhang, E.H. Abramson, D.G. Imre, *J. Chem. Phys.* 95 (1991) 6536.
- [17] D.G. Imre, J. Zhang, *Chem. Phys.* 139 (1989) 89.
- [18] N.E. Henriksen, J. Zhang, D.G. Imre, *J. Chem. Phys.* 89 (1988) 5607.
- [19] W. Fuß, W.E. Schmid, S.A. Trushin, *J. Chem. Phys.* 112 (2000) 8347.
- [20] S.A. Trushin, W. Fuß, K. Kosma, W.E. Schmid, *Appl. Phys. B* 85 (2006) 1.
- [21] K. Kosma, S.A. Trushin, W.E. Schmid, W. Fuß, *Opt. Lett.* 33 (2008) 723.
- [22] K. Kosma, S.A. Trushin, W. Fuß, W.E. Schmid, *J. Phys. Chem. A* 112 (2008) 7514.
- [23] K. Kosma, S.A. Trushin, W. Fuß, W.E. Schmid, *Phys. Chem. Chem. Phys.* (2009), doi:10.1039/B814201G.
- [24] K.B. Møller, N.E. Henriksen, A.H. Zewail, *J. Chem. Phys.* 113 (2000) 10477.
- [25] K.B. Møller, A.H. Zewail, *Chem. Phys. Lett.* 351 (2002) 281.
- [26] M.A. Pereira, P.E. Share, M.J. Sarisky, R.M. Hochstrasser, *J. Chem. Phys.* 94 (1991) 2513.
- [27] S.A. Trushin, K. Kosma, W. Fuß, W.E. Schmid, *Chem. Phys.* 347 (2008) 309.
- [28] W. Reuter, M. Perić, S.D. Peyerimhoff, *Mol. Phys.* 74 (1991) 569.
- [29] G. Herzberg, *Molecular spectra and molecular structure, Electronic Spectra and Electronic Structure of Polyatomic Molecules*, vol. 3, Van Nostrand Reinhold, New York, 1966.
- [30] E.J. Heller, *J. Chem. Phys.* 68 (1978) 3891.
- [31] M. Seel, W. Domcke, *J. Chem. Phys.* 95 (1991) 7806.
- [32] D. Azinovic, R. Bruckmeier, C. Wunderlich, H. Figger, G. Theodorakopoulos, I.D. Petsalakis, *Phys. Rev. A* 58 (1998) 1115.
- [33] S.A. Trushin, W.E. Schmid, W. Fuß, in preparation.
- [34] E. Kauppi, L. Halonen, *Chem. Phys. Lett.* 169 (1990) 393.